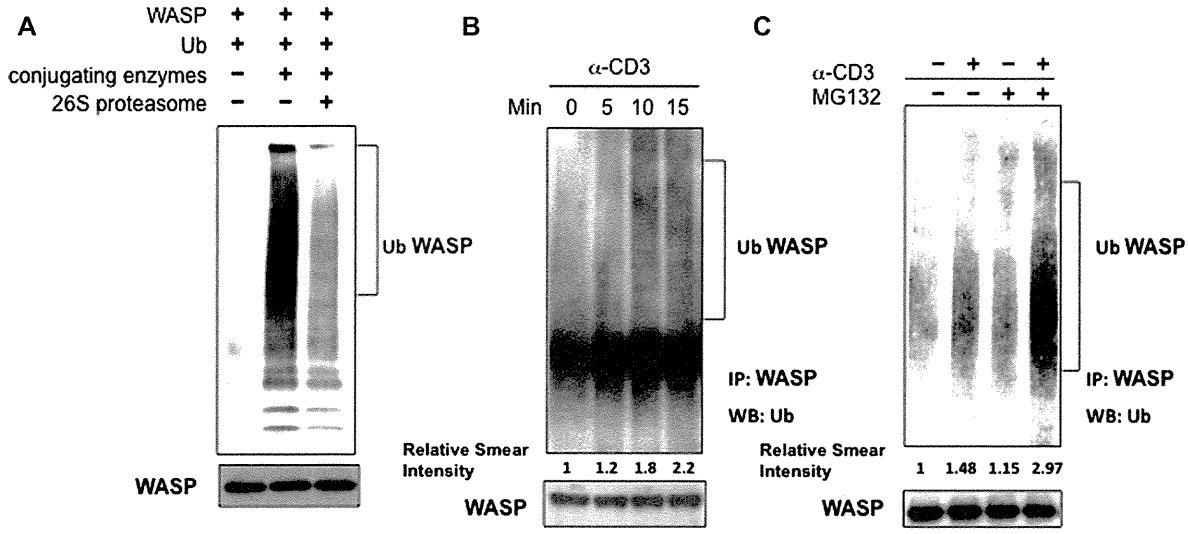

FIG 2. WASP is ubiquitinated and degraded by the 26S proteasome *in vitro* and in anti-CD3–stimulated Jurkat cells. **A,** Ubiquitination of *in vitro* translated purified WASP by ubiquitin-conjugating enzymes and its degradation by the 26S proteasome. Reaction mixtures were probed with anti-ubiquitin. **B,** Generation of ubiquitinated WASP in Jurkat T cells after stimulation with anti-CD3 mAb. WASP immunoprecipitates were probed with anti-ubiquitin mAb. Polyubiquitinated WASP appears as a smear. **C,** Protection of ubiquitinated WASP from degradation by the proteasome inhibitor MG132 in anti-CD3–stimulated Jurkat T cells. Similar results were obtained in Fig 2, *A* to *C*, in 4 independent experiments. The relative smear intensity in Fig 2, *B* and *C*, represents the mean of 4 experiments. *IP*, Immunoprecipitate; *Ub*, ubiquitin; *WB*, Western blot.

investigated whether Cbl proteins and WASP form a complex. WASP immunoprecipitates from Jurkat cell lysates were probed for c-Cbl and Cbl-b. c-Cbl, but not Cbl-b, coprecipitated weakly with WASP in unstimulated Jurkat T cells. TCR ligation increased the association of c-Cbl with WASP. It also induced the association of Cbl-b with WASP at 10 and 15 minutes after stimulation (Fig 3, *A*).

To investigate whether Cbl proteins act as E3 ubiquitin ligases for WASP, we transiently transfected 293T cells with plasmids coding for WT WASP, HA-tagged ubiquitin, FLAG-tagged c-Cbl, or FLAG-tagged Cbl-b. WASP coprecipitated with both c-Cbl and Cbl-b and was polyubiquitinated significantly more when co-transfected with ubiquitin, c-Cbl, and Cbl-b than with ubiquitin and empty vector (Fig 3, *B*).

To examine the role of Cbl-b in WASP ubiquitination after TCR ligation, we used purified T cells from spleens of *Cbl-b*$^{-/-}$ mice. Ubiquitination of WASP after TCR ligation was reduced, although not completely abrogated, in T cells from *Cbl-b*$^{-/-}$ mice (Fig 3, *C*), suggesting that WASP is a substrate for Cbl-b in antigen-stimulated T cells. We could not examine the role of c-Cbl on WASP ubiquitination after TCR ligation because we had no access to T cells from *c-Cbl*$^{-/-}$ mice.

WASP degradation after TCR/CD3 ligation limits TCR/CD3-driven F-actin assembly in T cells

WASP is important for F-actin assembly in T cells.[10] We examined whether WASP degradation after TCR/CD3 ligation regulates TCR/CD3-driven F-actin assembly. Purified T cells from WT and WASP-deficient mice were incubated for 6 hours with calpeptin or left untreated, washed and stimulated with anti-CD3 mAb, and cross-linked with a secondary antibody. The cells were then fixed, permeabilized, stained for F-actin with fluorescein isothiocyanate–conjugated phalloidin, and analyzed by means of flow cytometry. As previously reported, WASP-deficient T cells had a lower F-actin content than WT T cells.[16] TCR/CD3 ligation caused a parallel increase in F-actin levels in both WT and WASP-deficient T cells, which peaked at 5 minutes after stimulation and returned almost to baseline 10 minutes after stimulation. Pretreatment with calpeptin had no effect on F-actin content of the T cells at baseline or at 2 and 5 minutes after stimulation; however, it significantly increased the F-actin content of WT T cells at 10 minutes after anti-CD3 stimulation, maintaining it at almost the peak level achieved at 5 minutes after stimulation. In contrast, pretreatment with calpeptin had no effect on the F-actin content of WASP-deficient T cells 10 minutes after anti-CD3 stimulation. These results suggest that calpain-mediated WASP degradation limits the duration of F-actin assembly after TCR/CD3 ligation.

We next examined whether ubiquitination, which targets WASP for proteosomal degradation, regulates F-actin assembly after TCR/CD3 ligation. Because Cbl-b participates in WASP ubiquitination, we examined F-actin assembly in T cells deficient in Cbl-b. Baseline F-actin content and TCR-driven F-actin assembly were both significantly increased in T cells from c-Cbl-deficient mice compared with T cells from WT control animals (Fig 4, *B*). These results suggest that WASP degradation by ubiquitination regulates baseline and TCR-driven F-actin assembly.

DISCUSSION

Our results demonstrate that TCR ligation triggers the degradation of WASP by calpain-mediated cleavage and Cbl-mediated ubiquitination and subsequent proteasomal degradation. We present evidence that WASP degradation provides a mechanism for limiting the duration of TCR-driven assembly of F-actin.

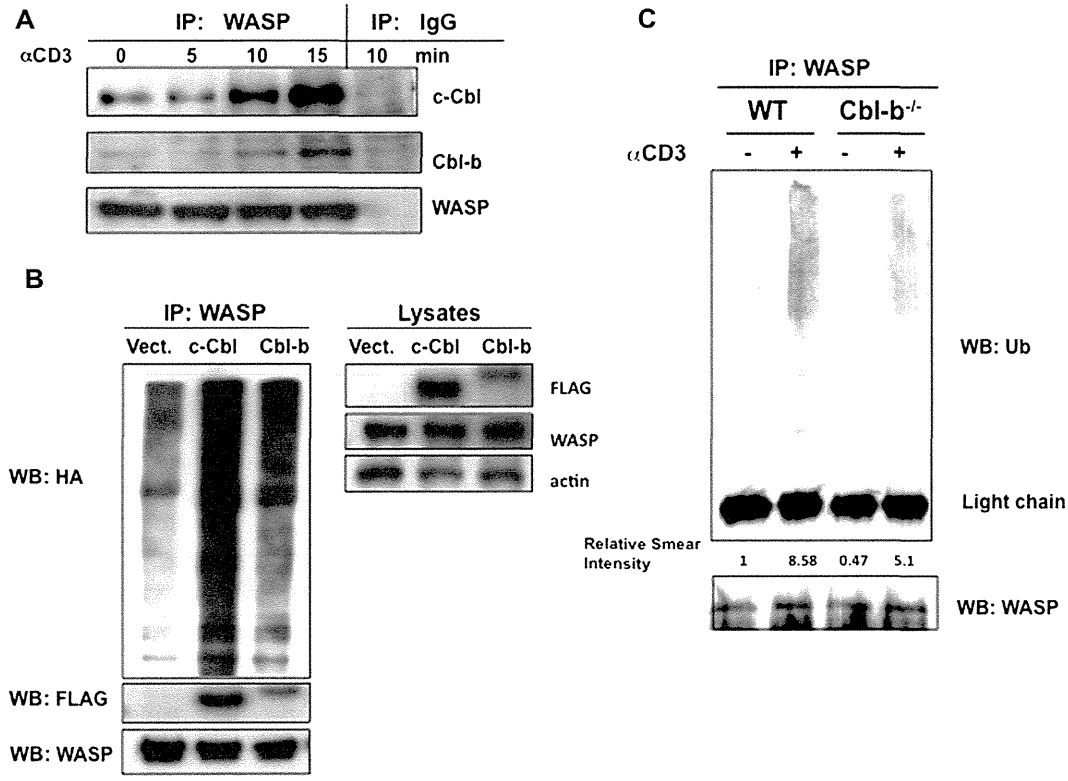

FIG 3. Cbl family E3 ubiquitin ligases associate with and ubiquitinate WASP after TCR ligation. **A,** Western blot analysis of WASP immunoprecipitates from anti-CD3–stimulated Jurkat T cells for c-Cbl and Cbl-b. IgG control antibody precipitates were prepared 10 minutes after anti-CD3 stimulation and used as controls. **B,** Ubiquitination of WASP in 293T cells transfected with WT WASP and HA-tagged ubiquitin plus either FLAG vector alone *(Vect.)*, FLAG-tagged c-Cbl, or FLAG-tagged Cbl-b. In the *left panel* WASP immunoprecipitates were probed for HA, FLAG, and WASP. In the *right panel* total lysates were probed for FLAG–c-Cbl or FLAG–Cbl-b, WASP, and actin. **C,** WASP ubiquitination after TCR ligation in T cells from *Cbl-b*$^{-/-}$ mice and WT control animals. WASP immunoprecipitates were probed for ubiquitin. Similar results were obtained in Fig 3, *A* to *C*, in 4 independent experiments. The relative smear intensity in Fig 3, *C*, represents the mean of 4 experiments. *IP*, Immunoprecipitate; *Ub*, ubiquitin; *WB*, Western blot.

TCR/CD3 ligation resulted in the degradation of a small fraction of WASP through calpain-mediated cleavage and the ubiquitin proteasome pathway. We estimated that approximately 5% of WASP is degraded after TCR/CD3 ligation. This is possibly an underestimate because the truncated 55-kDa WASP might be less stable than intact WASP. We could not detect a decrease in the levels of intact WASP in anti-CD3–activated T cells, probably because Western blotting is not sensitive enough to detect a small decrease in protein levels. We were unable to detect the cleaved, C-terminal, approximately 10-kDa fragment using an antibody to the C-terminus of WASP. This is most likely because such a small cleaved fragment would be rapidly degraded in the cell. Normally, WASP is protected from degradation by its partner, WIP.[16] The conformational changes in WASP induced by TCR signaling, which involve a change from an inactive to an active form capable of activating the Arp2/3 complex and F-actin polymerization, possibly increases the susceptibility of WASP to calpain cleavage and to ubiquitination and proteasomal degradation. The observation that WASP is degraded by calpain after TCR ligation is consistent with previous observations that WASP can be degraded in platelet lysates by calpain[29] and that *in vitro* translated WASP is a substrate for calpain I and II.[16] The increase in intracellular Ca^{++} concentration that follows TCR ligation could be the trigger for the Ca^{++}-dependent activation of calpain in anti-CD3–stimulated T cells.

Both c-Cbl and Cbl-b associated with WASP when overexpressed in 293T cells and acted as E3 ubiquitin ligases for WASP ubiquitination *in vitro*. More importantly, WASP ubiquitination after TCR ligation was impaired in Cbl-b-deficient T cells, implicating at least Cbl-b in WASP ubiquitination in T cells. Cbl family proteins act as negative regulators of TCR signaling by virtue of their ability to ubiquitinate LCK and ZAP-70,[33] which are upstream of WASP. Thus Cbl family members might regulate WASP activity indirectly by dampening TCR signaling upstream of WASP, as well as directly by ubiquitinating WASP and targeting it for degradation. Evidence has been presented that the activated WASP phosphorylated at Y291 is a target for ubiqutination.[34] We have also found that inhibition of the proteasome by MG132 increases the amount of tyrosine-phosphorylated WASP in anti-CD3–stimulated cells (see Fig E1 in this article's Online Repository at www.jacionline.org). This observation lends further support to the notion that activated WASP molecules are targets for degradation after TCR ligation.

It is not clear whether the interaction between WASP and c-Cbl and Cbl-b is direct or mediated by other proteins. It has been reported that c-Cbl associates with multiple proteins, which

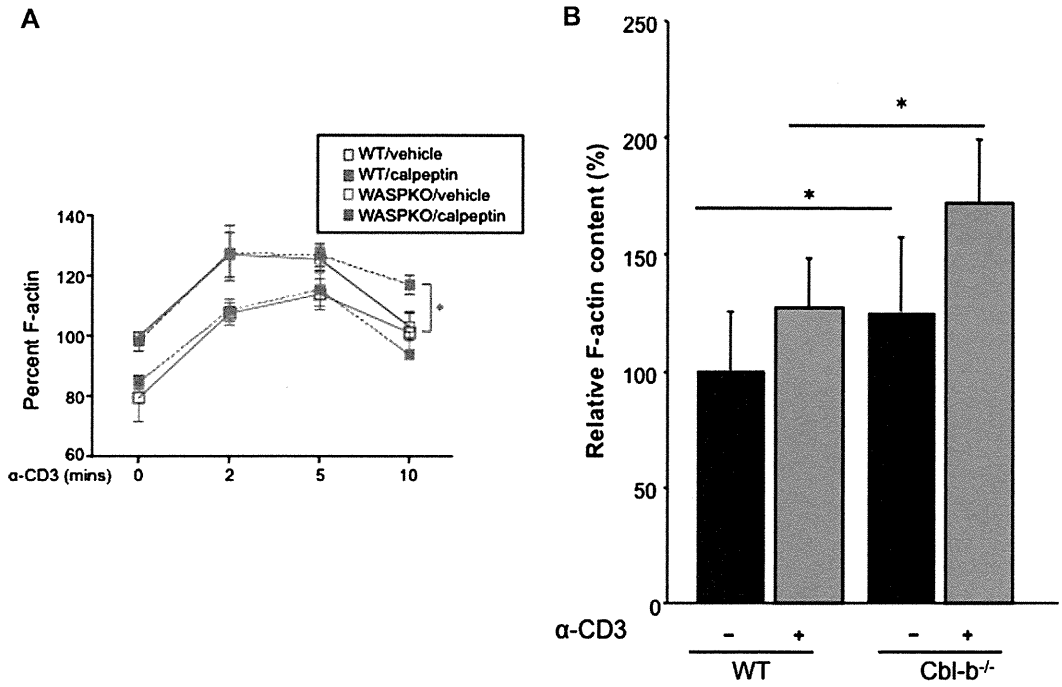

FIG 4. Effect of calpain inhibition and loss of Cbl on F-actin assembly in T cells. **A,** Effect of pretreatment of T cells from WT and WASP knockout mice with calpeptin on TCR-driven assembly of F-actin. Pretreatment with the vehicle dimethyl sulfoxide was used as a control. **B,** TCR-driven assembly of F-actin in T cells from *Cbl-b*$^{-/-}$ mice and WT control animals. T cells were stimulated with anti-CD3 for 10 minutes. Results are expressed as a percentage of the baseline F-actin content in unstimulated WT T cells and represent the means ± SDs of 3 independent experiments. *$P < .01$.

include tyrosine phosphorylated ZAP-70,[35] the adaptor proteins Nck[36] and Grb2[37] through their SH3 domains, CrkL through its SH2 domain,[38] Src tyrosine kinases through their SH3 domains,[39,40] and Vav and the p85 regulatory subunit of phosphatidylinositol-3-OH kinase through their SH2 domains.[41,42] Because these proteins are also reported to associate with WASP, its partner WIP, or both,[17,43] an indirect association of Cbl with WASP cannot be ruled out. Alternatively, c-Cbl and Cbl-b could directly interact with an activated form of WASP, such as tyrosine-phosphorylated WASP. Indeed, while this manuscript was in preparation, it was shown that WASP phosphorylation at tyrosine 291 after TCR activation results in recruitment of Cbl-b.[34]

Our data suggest that the degraded fraction of WASP includes activated WASP. This is supported by the observation that calpain inhibition and lack of the WASP-ubiquitinating E3 ligase Cbl-b resulted in more sustained F-actin assembly in WT T cells after TCR/CD3 ligation. The small fraction of WASP that is cleaved after TCR ligation could be important for F-actin polymerization because of its location close to the TCR. Indeed, we have shown previously that a fraction of WASP translocates together with a fraction of the TCR/CD3 complex to lipid rafts.[17] It is also well known that a fraction of WASP colocalizes with TCR molecules in the immune synapse (IS).[17,44,45] Cbl family molecules, which are also recruited to the IS, where they are activated by LCK and ZAP-70,[46,47] could ubiquitinate WASP molecules recruited to the IS, targeting them for degradation. The IS is a dynamic structure that constantly undergoes protein kinase Cθ–dependent dissolution and WASP/F-actin–dependent reformation of its peripheral supramolecular activation complex.[45] Protein kinase Cθ–dependent dissolution breaks the symmetry of the IS and allows T-cell motility. WASP/F-actin–dependent reformation of the IS is important for the sustained signaling that is necessary for IL-2 production. We speculate that cycles of TCR-triggered recruitment and activation of WASP in the IS followed by local degradation of the activated WASP might be important for IS dynamics and T-cell function.

The observation that baseline F-actin content was increased in *Cbl-b*$^{-/-}$ T cells, but not in calpeptin-treated T cells, suggests that under steady-state conditions, Cbl ubiquitination and proteasome degradation, but not calpain, degrade WASP molecules in activated in T cells. The observation that calpain inhibition had no effect on F-actin assembly in WASP-deficient T cells indicates that calpain regulates F-actin assembly by targeting WASP for degradation. These results strongly suggest that degradation of activated WASP by calpain and by the ubiquitin/proteasome pathway provide an important homeostatic mechanism for terminating signaling to the cytoskeleton after TCR ligation. Furthermore, WASP mutants that are resistant to ubiquitination are associated with enhanced T-cell activation, supporting the notion that WASP degradation limits TCR activation.[34]

Protein cleavage is used by prokaryotes and eukaryotes to activate or terminate signaling. Well-documented examples include the coagulation cascade, the complement activation cascade, degradation of the nuclear factor κB inhibitor IκBα, TNF receptor–associated factor 3, Argonaute, and voltage-gated calcium-channel proteins.[48-53] Degradation of activated WASP might regulate receptor signaling to the cytoskeleton not only in T cells but also in other hematopoietic cells. Such a control mechanism would avoid the potential pathology observed in patients with mutations that cause sustained WASP activation and manifest as X-linked neutropenia.

We thank K. A. Siminovitch, H. Gu, N. Ishii, and Y. Tanaka for reagents and mice.

Key message

- **TCR signaling causes WASP to be degraded by calpain and by Cbl-family members through ubiquitination and destruction by the proteasome, limiting TCR-driven assembly of F-actin.**

REFERENCES

1. Ochs HD, Rosen FS. The Wiskott-Aldrich syndrome. 2nd ed. New York: Oxford University Press; 2006.
2. Derry JMJ, Ochs HD, Francke U. Isolation of a novel gene mutated in Wiskott-Aldrich syndrome. Cell 1994;78:635-44.
3. Kwan SP, Hagemann TL, Radtke BE, Blaese RM, Rosen FS. Identification of mutations in the Wiskott-Aldrich syndrome gene and characterization of a polymorphic dinucleotide repeat at DXS6940, adjacent to the disease gene. Proc Natl Acad Sci U S A 1995;92:4706-10.
4. Anton IM, Jones GE, Wandosell F, Geha R, Ramesh N. WASP-interacting protein (WIP): working in polymerisation and much more. Trends Cell Biol 2007;17:555-62.
5. Higgs HN, Pollard TD. Activation by Cdc42 and PIP2 of Wiskott-Aldrich syndrome protein (WASp) stimulates actin nucleation by Arp2/3 complex. J Cell Biol 2000;150:1311-20.
6. Ramesh N, Anton IM, Hartwig JH, Geha RS. WIP, a protein associated with Wiskott-Aldrich syndrome protein, induces actin polymerization and redistribution in lymphoid cells. Proc Natl Acad Sci U S A 1997;94:14671-6.
7. Badour K, Zhang J, Siminovitch KA. Involvement of the Wiskott-Aldrich syndrome protein and other actin regulatory adaptors in T cell activation. Semin Immunol 2004;16:395-407.
8. Huang Y, Burkhardt JK. T-cell-receptor-dependent actin regulatory mechanisms. J Cell Sci 2007;120:723-30.
9. Thrasher AJ. WASp in immune-system organization and function. Nat Rev Immunol 2002;2:635-46.
10. Gallego MD, Santamaria M, Pena J, Molina IJ. Defective actin reorganization and polymerization of Wiskott-Aldrich T cells in response to CD3-mediated stimulation. Blood 1997;90:3089-97.
11. Snapper SB, Rosen FS, Mizoguchi E, Cohen P, Khan W, Liu C-H, et al. Wiskott-Aldrich Syndrome protein-deficient mice reveal a role for WASP in T but not B cell activation. Immunity 1998;9:81-91.
12. Zhang J, Shehabeldin A, da Cruz LA, Butler J, Somani AK, McGavin M, et al. Antigen receptor-induced activation and cytoskeletal rearrangement are impaired in Wiskott-Aldrich syndrome protein-deficient lymphocytes. J Exp Med 1999;190:1329-42.
13. Cory GO, Garg R, Cramer R, Ridley AJ. Phosphorylation of tyrosine 291 enhances the ability of WASp to stimulate actin polymerization and filopodium formation. J Biol Chem 2002;277:45115-21.
14. Rohatgi R, Nollau P, Ho HY, Kirschner MW, Mayer BJ. Nck and phosphatidylinositol 4,5-bisphosphate synergistically activate actin polymerization through the N-WASP-Arp2/3 pathway. J Biol Chem 2001;276:26448-52.
15. Torres E, Rosen MK. Contingent phosphorylation/dephosphorylation provides a mechanism of molecular memory in WASP. Mol Cell 2003;11:1215-27.
16. de la Fuente MA, Sasahara Y, Calamito M, Anton IM, Elkhal A, Gallego MD, et al. WIP is a chaperone for Wiskott-Aldrich syndrome protein (WASP). Proc Natl Acad Sci U S A 2007;104:926-31.
17. Sasahara Y, Rachid R, Byrne MJ, de la Fuente MA, Abraham RT, Ramesh N, et al. Mechanism of recruitment of WASP to the immunological synapse and of its activation following TCR ligation. Mol Cell 2002;10:1269-81.
18. Lanzi G, Moratto D, Vairo D, Masneri S, Delmonte O, Paganini T, et al. A novel primary human immunodeficiency due to deficiency in the WASP-interacting protein WIP. J Exp Med 2012;209:29-34.
19. Moratto D, Giliani S, Notarangelo LD, Mazza C, Mazzolari E, Notarangelo LD. The Wiskott-Aldrich syndrome: from genotype-phenotype correlation to treatment. Expert Rev Clin Immunol 2007;3:813-24.
20. Ochs HD, Notarangelo LD. Structure and function of the Wiskott-Aldrich syndrome protein. Curr Opin Hematol 2005;12:284-91.
21. Massaad MJ, Ramesh N, Le Bras S, Giliani S, Notarangelo LD, Al-Herz W, et al. A peptide derived from the Wiskott-Aldrich syndrome (WAS) protein-interacting protein (WIP) restores WAS protein level and actin cytoskeleton reorganization in lymphocytes from patients with WAS mutations that disrupt WIP binding. J Allergy Clin Immunol 2011;127:998-1005, e1-2.
22. Devriendt K, Kim AS, Mathijs G, Frints SG, Schwartz M, Van Den Oord JJ, et al. Constitutively activating mutation in WASP causes X-linked severe congenital neutropenia. Nat Genet 2001;27:313-7.
23. Ochs HD. Mutations of the Wiskott-Aldrich syndrome protein affect protein expression and dictate the clinical phenotypes. Immunol Res 2009;44:84-8.
24. Beel K, Cotter MM, Blatny J, Bond J, Lucas G, Green F, et al. A large kindred with X-linked neutropenia with an I294T mutation of the Wiskott-Aldrich syndrome gene. Br J Haematol 2009;144:120-6.
25. Westerberg LS, Meelu P, Baptista M, Eston MA, Adamovich DA, Cotta-de-Almeida V, et al. Activating WASP mutations associated with X-linked neutropenia result in enhanced actin polymerization, altered cytoskeletal responses, and genomic instability in lymphocytes. J Exp Med 2010;207:1145-52.
26. Kawai S, Minegishi M, Ohashi Y, Sasahara Y, Kumaki S, Konno T, et al. Flow cytometric determination of intracytoplasmic Wiskott-Aldrich syndrome protein in peripheral blood lymphocyte subpopulations. J Immunol Methods 2002;260:195-205.
27. Tanaka Y, Tanaka N, Saeki Y, Tanaka K, Murakami M, Hirano T, et al. c-Cbl-dependent monoubiquitination and lysosomal degradation of gp130. Mol Cell Biol 2008;28:4805-18.
28. Du W, Kumaki S, Uchiyama T, Yachie A, Yeng Looi C, Kawai S, et al. A second-site mutation in the initiation codon of WAS (WASP) results in expansion of subsets of lymphocytes in an Wiskott-Aldrich syndrome patient. Hum Mutat 2006; 27:370-5.
29. Shcherbina A, Miki H, Kenney DM, Rosen FS, Remold-O'Donnell E. WASP and N-WASP in human platelets differ in sensitivity to protease calpain. Blood 2001; 98:2988-91.
30. Chou HC, Anton IM, Holt MR, Curcio C, Lanzardo S, Worth A, et al. WIP regulates the stability and localization of WASP to podosomes in migrating dendritic cells. Curr Biol 2006;16:2337-44.
31. Bachmaier K, Krawczyk C, Kozieradzki I, Kong YY, Sasaki T, Oliveira-dos-Santos A, et al. Negative regulation of lymphocyte activation and autoimmunity by the molecular adaptor Cbl-b. Nature 2000;403:211-6.
32. Paolino M, Penninger JM. Cbl-b in T-cell activation. Semin Immunopathol 2010; 32:137-48.
33. Krawczyk C, Penninger JM. Molecular controls of antigen receptor clustering and autoimmunity. Trends Cell Biol 2001;11:212-20.
34. Reicher B, Joseph N, David A, Pauker MH, Perl O, Barda-Saad M. Ubiquitylation-dependent negative regulation of WASp is essential for actin cytoskeleton dynamics. Mol Cell Biol 2012;32:3153-63.
35. Lupher ML Jr, Reedquist KA, Miyake S, Langdon WY, Band H. A novel phosphotyrosine-binding domain in the N-terminal transforming region of Cbl interacts directly and selectively with ZAP-70 in T cells. J Biol Chem 1996;271: 24063-8.
36. Miyoshi-Akiyama T, Aleman LM, Smith JM, Adler CE, Mayer BJ. Regulation of Cbl phosphorylation by the Abl tyrosine kinase and the Nck SH2/SH3 adaptor. Oncogene 2001;20:4058-69.
37. Donovan JA, Ota Y, Langdon WY, Samelson LE. Regulation of the association of p120cbl with Grb2 in Jurkat T cells. J Biol Chem 1996;271:26369-74.
38. Gesbert F, Garbay C, Bertoglio J. Interleukin-2 stimulation induces tyrosine phosphorylation of p120-Cbl and CrkL and formation of multimolecular signaling complexes in T lymphocytes and natural killer cells. J Biol Chem 1998;273: 3986-93.
39. Reedquist KA, Fukazawa T, Panchamoorthy G, Langdon WY, Shoelson SE, Druker BJ, et al. Stimulation through the T cell receptor induces Cbl association with Crk proteins and the guanine nucleotide exchange protein C3G. J Biol Chem 1996;271:8435-42.
40. Tanaka S, Neff L, Baron R, Levy JB. Tyrosine phosphorylation and translocation of the c-cbl protein after activation of tyrosine kinase signaling pathways. J Biol Chem 1995;270:14347-51.
41. Jain SK, Langdon WY, Varticovski L. Tyrosine phosphorylation of p120cbl in BCR/abl transformed hematopoietic cells mediates enhanced association with phosphatidylinositol 3-kinase. Oncogene 1997;14:2217-28.
42. Tartare-Deckert S, Monthouel MN, Charvet C, Foucault I, Van Obberghen E, Bernard A, et al. Vav2 activates c-fos serum response element and CD69 expression but negatively regulates nuclear factor of activated T cells and interleukin-2 gene activation in T lymphocyte. J Biol Chem 2001;276:20849-57.
43. Anton IM, Lu W, Mayer BJ, Ramesh N, Geha RS. The Wiskott-Aldrich syndrome protein-interacting protein (WIP) binds to the adaptor protein Nck. J Biol Chem 1998;273:20992-5.
44. Cannon JL, Labno CM, Bosco G, Seth A, McGavin MH, Siminovitch KA, et al. Wasp recruitment to the T cell:APC contact site occurs independently of Cdc42 activation. Immunity 2001;15:249-59.
45. Sims TN, Soos TJ, Xenias HS, Dubin-Thaler B, Hofman JM, Waite JC, et al. Opposing effects of PKCtheta and WASp on symmetry breaking and relocation of the immunological synapse. Cell 2007;129:773-85.

46. Elly C, Witte S, Zhang Z, Rosnet O, Lipkowitz S, Altman A, et al. Tyrosine phosphorylation and complex formation of Cbl-b upon T cell receptor stimulation. Oncogene 1999;18:1147-56.
47. Wiedemann A, Muller S, Favier B, Penna D, Guiraud M, Delmas C, et al. T-cell activation is accompanied by an ubiquitination process occurring at the immunological synapse. Immunol Lett 2005;98:57-61.
48. Schenone M, Furie BC, Furie B. The blood coagulation cascade. Curr Opin Hematol 2004;11:272-7.
49. Forneris F, Wu J, Gros P. The modular serine proteases of the complement cascade. Curr Opin Struct Biol 2012;22:333-41.
50. Baud V, Derudder E. Control of NF-kappaB activity by proteolysis. Curr Top Microbiol Immunol 2011;349:97-114.
51. Bronevetsky Y, Villarino AV, Eisley CJ, Barbeau R, Barczak AJ, Heinz GA, et al. T cell activation induces proteasomal degradation of Argonaute and rapid remodeling of the microRNA repertoire. J Exp Med 2013;210:417-32.
52. Razani B, Reichardt AD, Cheng G. Non-canonical NF-kappaB signaling activation and regulation: principles and perspectives. Immunol Rev 2011;244:44-54.
53. De Jongh KS, Colvin AA, Wang KK, Catterall WA. Differential proteolysis of the full-length form of the L-type calcium channel alpha 1 subunit by calpain. J Neurochem 1994;63:1558-64.

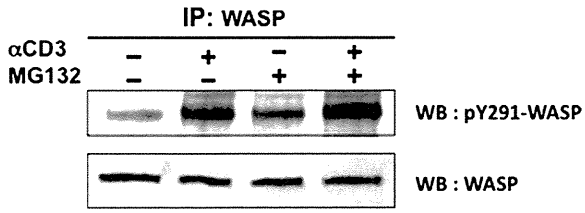

FIG E1. Tyrosine-phosphorylated WASP generated after TCR ligation is a target for proteasomal degradation. Effect of pretreatment of MG132 on the amount of tyrosine-phosphorylated WASP in anti-CD3–stimulated Jurkat T cells is shown. WASP immunoprecipitates were probed with anti-pY291-WASP antibody (Abcam). Similar results were obtained in 3 experiments. *IP*, Immunoprecipitate; *WB*, Western blot.

Gut Online First, published on November 7, 2012 as 10.1136/gutjnl-2012-303860

LETTER

Identification of novel missense *CTRC* variants in Japanese patients with chronic pancreatitis

We read with great interest the article by Paliwal *et al*[1] reporting the identification of novel missense variants in the chymotrypsin C (*CTRC*) gene in patients with tropical pancreatitis and idiopathic chronic pancreatitis (CP) in India. Because there might be geographical differences in the genetics of pancreatitis, we conducted screening of the *CTRC* gene in Japanese patients with CP. All the eight exons in the *CTRC* gene were directly sequenced in 506 patients with CP (244 alcoholic, 206 idiopathic, 35 hereditary and 21 familial) and 274 healthy controls as previously described.[1] This study was approved by the ethics committee of Tohoku University School of Medicine (article #2012-1-158). We identified five missense variants in patients with CP and one in controls (table 1).

Four variants were located in exon 7, 1 in exon 2, and 1 in exon 6. All missense variants were in a heterozygous form. Five of these six variants were novel ones. The c.86G>A (p.R29Q) and c.716C>G (p.S239C) variants were found in patients with alcoholic CP, whereas the c.715T>G (p.S239A) was found in a patient with idiopathic CP. The previously reported c.760C>T (p.R254W) variant was found in a patient with idiopathic CP, who also had the p.N34S variant in the serine protease inhibitor Kazal type I (*SPINK1*) gene in a heterozygous form. The c.739A>G (p.K247E) variant was found in a patient with alcoholic CP and two patients with idiopathic CP. The combined frequency of the missense *CTRC* variants was not statistically different between patients with CP (7/506) and controls (1/274) (p=0.27, Fisher's exact test). In addition to these missense variants, two synonymous variants, c.180C>T and c.285C>T, were found both in patients with CP and controls at the similar frequencies. Previous reports have shown an association of the *CTRC* variants with CP in Europe[2 3] and India.[1] In European cohorts, the microdeletion variant c.738_761del24 (p.K247_R254del) and the p.R254W, both located in exon 7, are the most common *CTRC* variants. In India, these variants are rare, and the c.217G>A (p.A73T) variant in exon 3 and the c.703G>A (p.V251I) variant are the most common ones.[1] These common variants in Europe and India were very rare in Japanese subjects, and only one patient with idiopathic CP had the p.R254W variant. Our results show that the spectrum and distribution of the *CTRC* variants in Japanese subjects with CP were different from those reported from Europe and India. In addition, the synonymous variant c.180C>T was common and was found in 32.7% and 27.2% of the patients with CP in India[1] and France,[3] respectively. This variant was significantly associated with CP (32.7% in patients vs 15.2% in controls) in India.[1] However, the c.180C>T variant is very rare in the Japanese population, further suggesting geographical differences in the distribution of the *CTRC* variants. It would be of interest to see the functional consequence of the missense variants identified in this study. Beer *et al*[4] have identified three different loss-of-function mechanisms caused by the *CTRC* variants: reduced secretion with associated endoplasmic reticulum stress, decreased catalytic activity, and degradation by trypsin. Obviously, further studies are required to establish the role of the novel missense variants in the pathogenesis of pancreatitis.

Table 1 *CTRC* variants in the exons identified in this study

CTRC Variants	Total CP (%)	Alcoholic CP (%)	Non-alcoholic CP (%)	Controls (%)	p Value (Total CP vs Controls)
Missense variants					
Exon 2					
c.86G>A (p.R29Q)	1/506 (0.2)	1/244 (0.4)	0/262 (0)	0/274 (0)	>0.99
Exon 6					
c.627C>G (p.I209M)	0/506 (0)	0/244 (0)	0/262 (0)	1/274 (0.4)	0.35
Exon 7					
c.715T>G (p.S239A)	1/506 (0.2)	0/244 (0)	1/262 (0.4)	0/274 (0)	>0.99
c.716C>G (p.S239C)	1/506 (0.2)	0/244 (0)	1/262 (0.4)	0/274 (0)	>0.99
c.739A>G (p.K247E)	3/506 (0.6)	1/244 (0.4)	2/262 (0.8)	0/274 (0)	0.56
c.760C>T (p.R254W)	1/506 (0.2)	0/244 (0)	1/262 (0.4)	0/274 (0)	>0.99
CTRC missense variants total	7/506 (1.4)	2/244 (0.8)	5/262 (2.0)	1/274 (0.4)	0.27
Synonymous variants					
c.180C>T (p.(=))	1/506 (0.2)	1/244 (0.4)	0/262 (0)	0/274 (0)	>0.99
c.285C>T (p.(=))	51/506 (10.1)	23 /244 (9.4)	28/262 (10.7)	24/274 (8.8)	0.61

Nomenclature follows the guidelines recommended by the Human Genome Variation Society (http://www.hgvs.org/): cDNA-based numbering with A of the ATG translational initiation codon ascribed +1. GenBank accessions NM_007272.2 and NC_ 000001.10 were used as the reference mRNA and genomic DNA sequences, respectively.
CP, chronic pancreatitis.

Atsushi Masamune, Eriko Nakano, Kiyoshi Kume, Yoichi Kakuta, Hiroyuki Ariga, Tooru Shimosegawa

Division of Gastroenterology, Tohoku University Graduate School of Medicine, Sendai, Japan

Correspondence to Dr Atsushi Masamune, Division of Gastroenterology, Tohoku University Graduate School of Medicine, 1-1 Seiryo-machi, Aoba-ku, Sendai 980-8574, Japan;
amasamune@med.tohoku.ac.jp

Contributors AM and TS designed the project. AM, EN, KK, YK and HA performed the experiments. AM and EN wrote the manuscript. AM, EN and KK contributed equally to this work.

Financial supports This work was supported in part by a Grant-in-Aid from Japan Society for the Promotion of Science (23591008 and 23659392), and by the Ministry of Health, Labour, and Welfare of Japan.

Competing interests None.

Patient consent Obtained.

Provenance and peer review Not commissioned; internally peer reviewed.

Gut 2012;**0**:1. doi:10.1136/gutjnl-2012-303860

REFERENCES

1. **Paliwal S,** Bhaskar S, Mani KR, *et al*. Comprehensive screening of chymotrypsin C (CTRC) gene in tropical calcific pancreatitis identifies novel variants. *Gut* Published Online First: 12 May 2012. doi:10.1136/gutjnl-2012-302448.
2. **Rosendahl J,** Witt H, Szmola R, *et al*. Chymotrypsin C (CTRC) variants that diminish activity or secretion are associated with chronic pancreatitis. *Nat Genet* 2008;**40**:78–82.
3. **Masson E,** Chen JM, Scotet V, *et al*. Association of rare chymotrypsinogen C (CTRC) gene variations in patients with idiopathic chronic pancreatitis. *Hum Genet* 2008;**123**:83–91.
4. **Beer S,** Zhou J, Szabó A, *et al*. Comprehensive functional analysis of chymotrypsin C (CTRC) variants reveals distinct loss-of-function mechanisms associated with pancreatitis risk. *Gut* Published Online First: 1 September 2012. doi:10.1136/gutjnl-2012–303090.

GUT

Identification of novel missense *CTRC* variants in Japanese patients with chronic pancreatitis

Atsushi Masamune, Eriko Nakano, Kiyoshi Kume, et al.

Gut published online November 7, 2012
doi: 10.1136/gutjnl-2012-303860

LETTERS

PRSS1 c.623G>C (p.G208A) variant is associated with pancreatitis in Japan

We read with great interest the article by Schnúr *et al*[1] reporting the functional effects of 13 serine protease 1 (*PRSS1*) variants found in sporadic chronic pancreatitis (CP). They reported that five mutants, including p.G208A, showed reduced secretion, suggesting that these variants might increase the risk of pancreatitis related to mutation-induced misfolding and consequent endoplasmic reticulum stress. The pathological role of these variants might be strengthened by their association with pancreatitis cohorts, but such information is scarce. Interestingly, the c.623G>C (p.G208A) variant has been reported only in Asian subjects: a 12-year-old Asian man with CP, a Korean child with recurrent pancreatitis and a 7-year-old Korean child with necrotising acute pancreatitis.[2 3] We therefore conducted screening of the *PRSS1* p.G208A variant in Japanese patients with CP. All of the exons and the flanking regions in the *PRSS1* gene were amplified by PCR and directly sequenced in 484 patients with CP (232 alcoholic, 198 idiopathic, 34 hereditary and 20 familial) and 411 healthy controls. In addition, all subjects were screened for mutations in the serine protease inhibitor Kazal type 1 (*SPINK1*) and chymotrypsin C (*CTRC*) genes. All subjects were Japanese. This study was approved by the Ethics Committee of Tohoku University School of Medicine. The *PRSS1* c.623G>C (p.G208A) variant was found in eight patients with alcoholic CP, nine patients with idiopathic CP and one patient with hereditary CP (table 1). The frequency of a common variant, c.738T>C (p.N246=), was not different between the patients with CP (235/484) and the controls (186/411) (p=0.25). Of the nine patients with idiopathic CP carrying the p.G208A variant, seven patients developed pancreatitis before the age of 20 years (the age at onset in these seven patients was 1, 2, 7, 11, 12, 15 and 19 years). Two patients (a patient with alcoholic CP whose age at onset was 28 years and a patient with idiopathic CP whose age at onset was 12 years) carrying the p.G208A variant also had the c.86G>A (p.R29Q) variant in the *CTRC* gene.[4] One patient with idiopathic CP carrying the p.G208A variant also had the c.101A>G (p.N34S) variant in the *SPINK1* gene. The other 15 patients carrying the p.G208A variant did not have the *PRSS1* c.365G>A (p.R122H), *PRSS1* c.86A>T (p.N29I), *SPINK1* c.101A>G (p.N34S) or *SPINK1* c.194+2T>C (IVS3+2T>C) variants. In a previous report,[3] a patient with pancreatitis carrying the p.G208A variant had the p.F508del and p.Q1352H mutations in the cystic fibrosis transmembrane conductance regulator (*CFTR*) gene. However, none of our subjects carrying the p.G208A variant had these mutations in the *CFTR* gene. The frequency of the p.G208A variant was higher in patients with CP (18/484) than in controls (1/411) (p<0.001; OR 15.8; 95% CI 2.1 to 119.2). The differences were still significant even if the patients were stratified based on the aetiology (p=0.002 for alcoholic CP vs controls, and p<0.001 for idiopathic CP vs controls). Our results showed that the *PRSS1* p.G208A variant is associated with CP in Japan. To our knowledge, this is the first *PRSS1* variant found in association with alcoholic CP. The risk conferred by the p.G208A variant seemed lower than that by the *PRSS1* 'classic mutation' p.R122H, and the p.G208A variant might require other (genetic, alcoholic or environmental) factors to reach the threshold for the development of CP. This notion might be supported by the association of this variant with alcoholic CP and by the presence of the *CTRC* p.R29Q and the *SPINK1* p.N34S variants in some patients. On the other hand, taken together with the previous reports of this variant only in Asian subjects, this variant might be a unique genetic background of pancreatitis in Asia.

Atsushi Masamune, Eriko Nakano, Kiyoshi Kume, Tetsuya Takikawa, Yoichi Kakuta, Tooru Shimosegawa

Division of Gastroenterology, Tohoku University Graduate School of Medicine, Sendai, Japan

Correspondence to Dr Atsushi Masamune, Division of Gastroenterology, Tohoku University Graduate School of Medicine, 1-1 Seiryo-machi, Aoba-ku, Sendai 980-8574, Japan; amasamune@med.tohoku.ac.jp

Contributors AM and ST designed the project. AM, EN, KK, TT, and YK performed the experiments. AM wrote the manuscript.

Funding This work was supported in part by Grant-in-Aid from the Japan Society for the Promotion of Science (#23591008) and by the Ministry of Health, Labour and Welfare of Japan.

Competing interests None.

Ethics approval The Ethics Committee of Tohoku University School of Medicine.

Provenance and peer review Not commissioned; externally peer reviewed.

To cite Masamune A, Nakano E, Kume K, *et al*. *Gut* 2014;**63**:366.

Received 19 March 2013
Accepted 19 April 2013
Published Online First 17 May 2013

▶ http://dx.doi.org/10.1136/gutjnl-2012-303860
▶ http://dx.doi.org/10.1136/gutjnl-2012-304331

Gut 2014;**63**:366. doi:10.1136/gutjnl-2013-304925

Table 1 Frequency of the PRSS1 c.623G>C (p.G208A) variant in Japanese patients with CP

Aetiology	Frequency (%)	OR (95% CI)	p Value (vs controls)*
Alcoholic	8/232 (3.4)	14.6 (1.8 to 117.8)	0.002
Idiopathic	9/198 (4.5)	19.5 (2.5 to 155.2)	<0.001
Hereditary	1/34 (2.9)	12.4 (0.7 to 203.2)	0.15
Familial	0/20 (0)	1.0 (1.0 to 1.0)	>0.99
Total CP	18/484 (3.7)	15.8 (2.1 to 119.2)	<0.001
Controls	1/411 (0.2)	–	–

*Fisher's exact test.
CP, chronic pancreatitis.

REFERENCES

1 Schnúr A, Beer S, Witt H, *et al*. Functional effects of 13 rare PRSS1 variants presumed to cause chronic pancreatitis. *Gut*. 2014;63:337–343.
2 Lee YJ, Kim KM, Choi JH, *et al*. High incidence of PRSS1 and SPINK1 mutations in Korean children with acute recurrent and chronic pancreatitis. *J Pediatr Gastroenterol Nutr* 2011;52:478–81.
3 Keiles S, Kammesheidt A. Identification of CFTR, PRSS1, and SPINK1 mutations in 381 patients with pancreatitis. *Pancreas* 2006;33:221–7.
4 Masamune A, Nakano E, Kume K, *et al*. Identification of novel missense CTRC variants in Japanese patients with chronic pancreatitis. *Gut* 2013;62:653–4.

GUT

PRSS1 c.623G>C (p.G208A) variant is associated with pancreatitis in Japan

Atsushi Masamune, Eriko Nakano, Kiyoshi Kume, et al.

Gut 2014 63: 366 originally published online May 17, 2013
doi: 10.1136/gutjnl-2013-304925

RESEARCH ARTICLE

AMERICAN JOURNAL OF medical genetics PART A

Clinical Consequences in Truncating Mutations in Exon 34 of *NOTCH2*: Report of Six Patients With Hajdu–Cheney Syndrome and a Patient With Serpentine Fibula Polycystic Kidney Syndrome

Yoko Narumi,[1]* Byung-Joo Min,[2] Kenji Shimizu,[3] Itsuro Kazukawa,[4] Kiyoko Sameshima,[5] Koichi Nakamura,[6] Tomoki Kosho,[1] Yumie Rhee,[7] Yoon-Sok Chung,[8] Ok-Hwa Kim,[9] Yoshimitsu Fukushima,[1] Woong-Yang Park,[2] and Gen Nishimura[10]

[1]Department of Medical Genetics, Shinshu University School of Medicine, Matsumoto, Japan

[2]Departments of Biomedical Sciences, Seoul National University College of Medicine, Seoul, Korea

[3]Division of Medical Genetics, Saitama Children's Medical Center, Saitama, Japan

[4]Division of Endocrinology, Chiba Children's Hospital, Chiba, Japan

[5]Division of Medical Genetics, Gunma Children's Medical Center, Shibukawa, Japan

[6]Department of Orthopedics, Shinshu University School of Medicine, Matsumoto, Japan

[7]Department of Internal Medicine, Endocrine Research Institute, Yonsei University College of Medicine, Seoul, Korea

[8]Department of Endocrinology and Metabolism, Ajou University School of Medicine, Suwon, Korea

[9]Department of Radiology, Ajou University School of Medicine, Suwon, Korea

[10]Department of Pediatric Imaging, Tokyo Metropolitan Children's Medical Center, Tokyo, Japan

Manuscript Received: 3 March 2012; Manuscript Accepted: 11 October 2012

It is debatable whether Hajdu–Cheney syndrome (HCS) and serpentine fibula-polycystic kidney syndrome (SFPKS) represent a single clinical entity with a variable degree of expression or two different entities, because both disorders share common clinical and radiological manifestations, including similar craniofacial characteristics, and defective bone mineralization. Since it was shown that heterozygous truncating mutations in *NOTCH2* are responsible for both HCS and SFPKS, 37 patients with HCS and four patients with SFPKS are reported. To elucidate the clinical consequences of *NOTCH2* mutations, we present detailed clinical information for seven patients with truncating mutations in exon 34 of *NOTCH2*, six with HCS and one with SFPKS. In addition, we review all the reported patients whose clinical manifestations are available. We found 13 manifestations including craniofacial features, acroosteolysis, Wormian bones, and osteoporosis in >75% of *NOTCH2*-positive patients. Acroosteolysis was observed in two patients with SFPKS and bowing fibulae were found in two patients with HCS. These clinical and molecular data would support the notion that HCS and SFPKS are a single disorder.

Key words: Hajdu–Cheney syndrome; serpentine fibula-polycystic kidney syndrome; NOTCH2; osteolysis; osteoporosis

How to Cite this Article:
Narumi Y, Min B-J, Shimizu K, Kazukawa I, Sameshima K, Nakamura K, Kosho T, Rhee Y, Chung YS, OH Kim, Fukushima Y, Park WY, Nishimura G. 2013. Clinical consequences in truncating mutations in exon 34 of *NOTCH2*: Report of six patients with Hajdu–Cheney syndrome and a patient with serpentine fibula polycystic kidney syndrome.
Am J Med Genet Part A 161A:518–526.

Additional supporting information may be found in the online version of this article.

Grant sponsor: Research on Grant-in-Aid, Ministry of Education, Culture, Sports, Science and technology, Japan; Grant numbers: 22790972, 24791844; Grant sponsor: The Korea Healthcare Technology R&D Project, Ministry for Health, Welfare and Family Affairs, Republic of Korea; Grant number: A080588.

Yoko Narumi, Byung-Joo Min, and Woong-Yang Park contributed equally to this work.

*Correspondence to:
Yoko Narumi, M.D., Ph.D., Department of Medical Genetics, Shinshu University School of Medicine, 3-1-1 Asahi, Matsumoto 390-8621, Japan.
E-mail: ynarumi@shinshu-u.ac.jp

Article first published online in Wiley Online Library (wileyonlinelibrary.com): 7 February 2013
DOI 10.1002/ajmg.a.35772

INTRODUCTION

Hajdu–Cheney syndrome (HCS) [OMIM#102500] is a rare autosomal dominant disorder, which is characterized by short stature, craniofacial anomalies, abnormal dentition, joint hypermobility, hearing impairment, defective bone mineralization, and progressive bone resorption, including progressive osteoporosis, multiple Wormian bones, progressive basilar invagination, and acroosteolysis [Brennan and Pauli, 2001]. HCS shares common manifestations with serpentine fibula-polycystic kidney syndrome (SFPKS) [OMIM#600330] which is characterized by facial dysmorphism that resembles HCS, short stature, polycystic kidneys, hearing impairment, bowed forearms, and elongated and S-shaped fibulae [Exner, 1988; Majewski et al., 1993]. It debatable whether HCS and SFPKS represent a single clinical entity with a variable degree of expression or two different entities [Kaplan et al., 1995; Ramos et al., 1998; Currarino, 2009; Takatani et al., 2009].

It has recently been demonstrated that heterozygous truncating mutations in *NOTCH2* are responsible for both HCS and SFPKS. To date, 37 patients with HCS and four patients with SFPKS have been reported with *NOTCH2* mutations [Isidor et al., 2011a,b; Majewski et al., 2011; Simpson et al., 2011; Gray et al., 2012]. *NOTCH2* encodes a single-pass transmembrane protein from the NOTCH receptor family (NOTCH1–NOTCH4 in mammals). It is intriguing that both HCS and SFPKS are caused by nonsense or frameshift mutations in the proline-glutamic acid-serine-threonine-rich (PEST) domain of *NOTCH2*. The PEST domain is essential for the proteasomal degradation of the Notch intracellular domain (NICD) and is located at the C terminus of the receptor. It is assumed that HCS or SFPKS-related *NOTCH2* mutations escape nonsense-mediated mRNA decay and cause gain-of-function effects [Simpson et al., 2011]. In murine models, the activation of Notch signaling arrests the commitment of pluripotent precursors to the osteoblastic lineage, and suppresses osteoblast differentiation [Zanotti and Canalis, 2012].

To elucidate clinical consequences of truncating mutations in exon 34 of *NOTCH2*, we present detailed clinical information of seven patients with *NOTCH2* mutations, six with HCS and one with SFPKS and clinical review of all reported patients whose clinical manifestations are available. This investigation may help us to decide whether the two conditions are distinct disorders or a single disorder.

CLINICAL REPORTS

Patient 1

Patient 1, a Japanese girl now 2 years of age, was the second child born to healthy nonconsanguineous parents. Bowed femurs were detected by prenatal ultrasonography at 25 weeks of gestation. She was delivered by cesarean at 37 weeks of gestation. Her birth length was 46 cm (10th centile of Japanese girls), weight 3,114 g (50th–75th centile of Japanese girls), occipital frontal circumference (OFC) of 35.5 cm (>97th centile of Japansese girl). Her apgar score was 3 at 1 min, and she received oxygen inhalation therapy because of respiratory insufficiency. Radiographs detected bowing of the femur, tibiae, and fibulae; deformation of the radii and ulnae; and a fracture line in the right femur. Echocardiography indicated a patent ductus arteriosus and trivial aortic regurgitation. Abdominal ultrasonography revealed bilateral polycystic kidneys.

At 3 months, she presented with a large anterior fontanelle ($3.5 \times 3.5\ cm^2$), diastasis of the sagittal suture, arched eyebrows, shallow orbit, mild proptosis, hypertelorism, broad nasal bridge, long philtrum, thin upper lip vermilion, micrognathia (Fig. 1A), a bifid uvula, and a short neck. Hearing impairment was detected with a threshold of 60 dB in the auditory brainstem response (ABR). A fiber optic laryngoscope detected laryngomalacia. Cranial magnetic resonance imaging (MRI) showed mild hydorocephalus at 10 months of age. The radiological findings included Wormian bones, patent cranial sutures, delayed calvarial ossification (Fig. 2A), generalized osteopenia with mild scoliosis (Fig. 3A), and acroosteolysis of both hands (Fig. 4A), which was first identified at 1 year and 6 months of age. Mildly bowed tibiae and serpentine fibulae were observed (Fig. 4B,C). The right fibula and left fifth metacarpal was fractured at 2 years of age. At 2 years and 8 months, her height was 81.2 cm (<3rd centile), weight 9.8 kg (<3rd centile), and OFC 49.5 cm (75th–90th centile). She showed developmental retardation with a developmental quotient (DQ) of 52 at 2 years and 7 months, and she was fed by a tube until 2 years and 4 months because of poor feeding.

Patient 2

Patient 2 was a Japanese girl who is now 14 years of age. Part of her medical history has been reported previously [Takatani et al., 2009]. At birth, she presented with exophthalmos, depression of the nasal tip, long philtrum, low-set ears, micrognathia, and a patent ductus arteriosus. Subsequently, she was found to have a submucous cleft palate, conductive hearing impairment, early loss of teeth, hydrocephalus, and platybasia. At 5 months of age, she was noted with optic nerve abnormal whiteness. She was diagnosed with bilateral optic nerve atrophy secondary to hydrocephalus. Renal ultrasonography detected normal kidneys. She experienced a left ulna and radius fracture at 6 years of age and two lumbar vertebral fractures at 13 years of age. Radiological findings including mild metaphyseal undermodeling of the long bones, bowing of the fibulae and ulnae, dislocation of the elbow joints, and a pseudofracture of the right fibula were reported previously. In addition, radiographs detected multiple Wormian bones, bathrocephaly (Fig. 2B), acroosteolysis of the distal phalanges (Fig. 4D), and generalized osteoporosis with vertebral compression fractures and thoracolumbar kyphosis (Fig. 3B). At 9 years of age, she reported headache, emesis, and gait difficulties. Cranial MRI showed platybasia with basilar invagination, progressive hydrocephalus, medullary kinking, and syringomyelia. She underwent surgery comprising a fenestration in the floor of the third ventricle, foramen magnum augmentation, and a ventriculoperitoneal shunt to improve symptoms. She exhibited developmental retardation with a DQ of 64 at 2 years and 6 months of age. At 14 years of age, her height was 126 cm (<3rd centile of Japanese girls) and her weight was 27 kg (<3rd centile of Japanese girls). She currently uses a wheelchair because of gait difficulties.

FIG. 1. Facial photographs. Patient 1 with arched eyebrows at 3 months of age (A). Patient 3 at 1 month; synophyrys was not noted (B), but recognized at 2 years (C). Patient 4 showed synophyrys in infancy (D), 3 years of age (E), and coarse hair and skins at 31 years of age (F).

Patient 3

Patient 3, a Japanese girl who is now 2 years of age, was the first child born to healthy nonconsanguineous parents. Pregnancy was associated with polyhydramnios. Prenatal ultrasonography revealed a hypoplastic left heart. She was born at 37 weeks of gestation. Her birth length was 47 cm (25th centile of Japanese girls), weight 2,952 g (50th centile of Japanese girls), and OFC 34.5 cm (90th centile of Japanese girls). Cardiac ultrasonography at birth showed hypoplastic left ventricle, subaortic stenosis, coarctation of aorta, and patent ductus arteriosus. She showed pulmonary hypertension and required oxygen therapy. At 30 months of age, her height was 81.2 cm (<3rd centile), weight 9.8 kg (<3rd centile), and OFC 48.6 cm (75th centile). Her left ventricle formation was improved with age. However, she presented with severe pulmonary hypertension and coarctation of aorta. She had a facial dysmorphism and rounded nails (Fig. 1B,C). Radiographs detected Wormian bones in the lambdoidal sutures (Fig. 2C) and mild bowing of the tibiae was evident. However, neither acroosteolysis nor osteoporosis was apparent (Figs. 3C and 4E,F) and polycystic kidney was not detected by renal ultrasonography. She exhibited normal development.

Patient 4

Patient 4 is now a 31-year-old Japanese woman. Her birth weight was 3,900 g (>97th centile of Japanese females). In her childhood, she presented with thick eyebrows, a short nose, a long philtrum, and micrognathia (Fig. 1D,E). Her development was normal. In her early elementary school years, she presented short fingers with rounded tips. The delayed loss of primary teeth and malposition of teeth were also observed. At 14 years of age, hallux valgus and distal interphalangeal joint contracture were noted and chronic back pain and stiff shoulders were also observed. She has had irregular menstrual cycle from menarche; thus, was suspected to have anovulomenorrhea, but she became pregnant and delivered a healthy son at age 28 years of age.

At 30 years of age, her height was 156 cm (50th centile) and weight 51 kg (50th centile). She had distinctive facial features

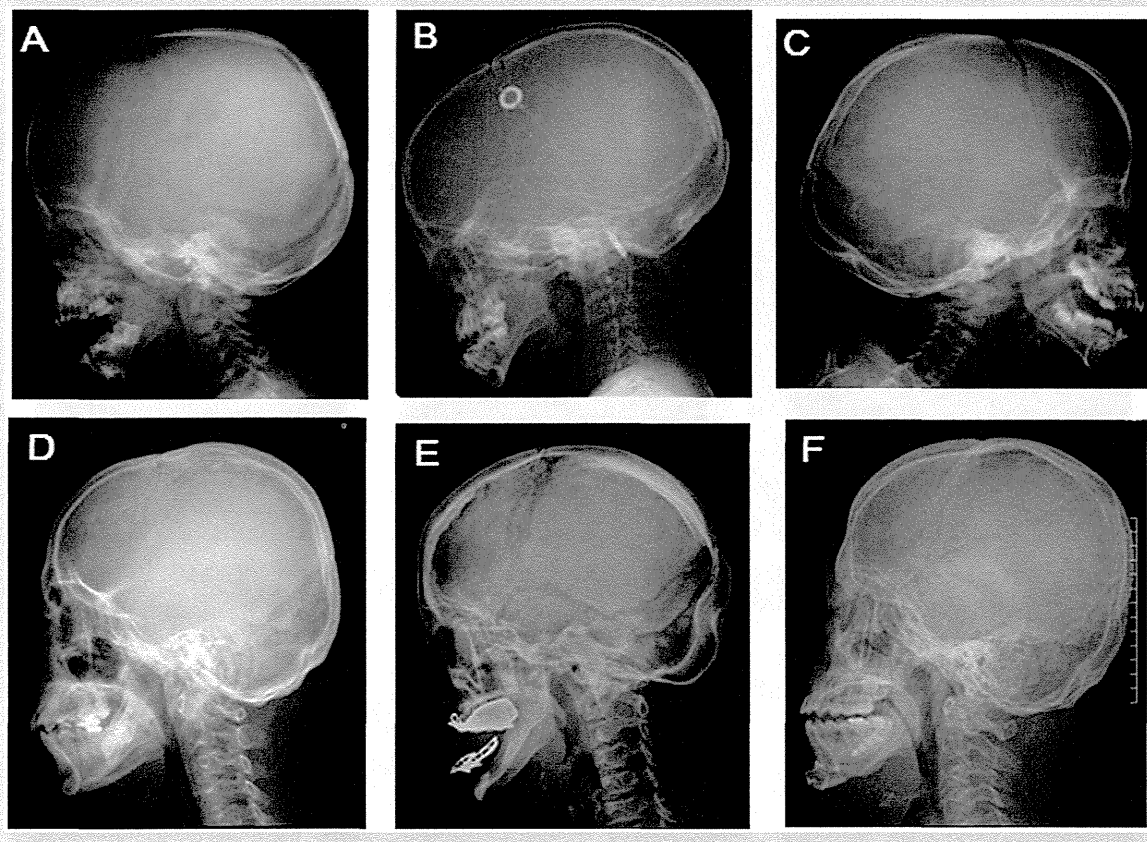

FIG. 2. Lateral skull radiographs. All patients showed Wormian bones. A: Patient 1 at 2 years and 11 months of age. B: Patient 2 at 13 years of age. C: Patient 3 at 2 years of age. D: Patient 4 at 31 years of age. E: Patient 5 at 41 years of age. F: Patient 6 at 20 years of age.

(Fig. 1F). Radiographs showed Wormian bone at the lambdoidal sutures (Fig. 2C) and acroosteolysis in the hands and feet (Fig. 4G,I), although osteoporosis and compression fractures were not noted (Fig. 3D). The bone mineral density of the lumbar spine was 0.873 g/cm^2 according to dual-energy X-ray absorptiometry, which corresponded to a T score of −2.0. The urine *N*-telopeptide of collagen type I, an osteoclast marker, was normal at 20.5 nmol BCE/mmolCr (normal values for premenopausal females = 9.3–54.3). The expression of the osteoblast marker serum bone-specific alkaline phosphatase (BAP) was also normal at 22.8 U/L. She did not display early loss of permanent teeth, pathological fractures, or any hearing or visual impairments.

Patient 5

Patient 5, a Korean woman, now 41 years of age has been described previously [Hwang et al., 2011]. She presented with mid-facial hypoplasia, micrognathia, short hands with pseudo-clubbing at the finger tip, malocclusion and loss of teeth, and patent ductus arteriosus. Her height was 139 cm (<3rd centile of Korean females). She had persistent pain in both hands and feet, and intermittent back pain. Radiographs showed Wormian bones with persistent patent cranial sutures, bathrocephaly (Fig. 2E), osteoporosis without compression fractures in the spine (Fig. 3E), and acroosteolysis in both hands and feet. The bone mineral density of her lumbar spine was 0.678 g/cm^2 according to dual-energy X-ray absorptiometry, which corresponded to T scores of −3.0.

Patient 6

Patient 6, a Korean man, now 20 years of age has been described previously [Han et al., 2010]. His developmental history was unremarkable. He presented with bushy eyebrows, mid-facial flattening with a wide nose, micrognathia, and distal clubbing fingers. At 19 years of age, his height was 168 cm (25th centile of Korean males). He underwent an operation for malocclusion of the teeth. He developed slow, progressive back pain and was found to have multiple spinal fractures and osteoporosis. Radiographs showed Wormian bones in the lambdoidal suture (Fig. 2F), osteoporosis with non-traumatic compression fractures throughout the lower thoracic and lumbar spine (Fig. 3F), and bilateral symmetrical acroosteolysis of the hands (Fig. 4I) and feet. The bone densitometry of the first lumbar vertebral body was

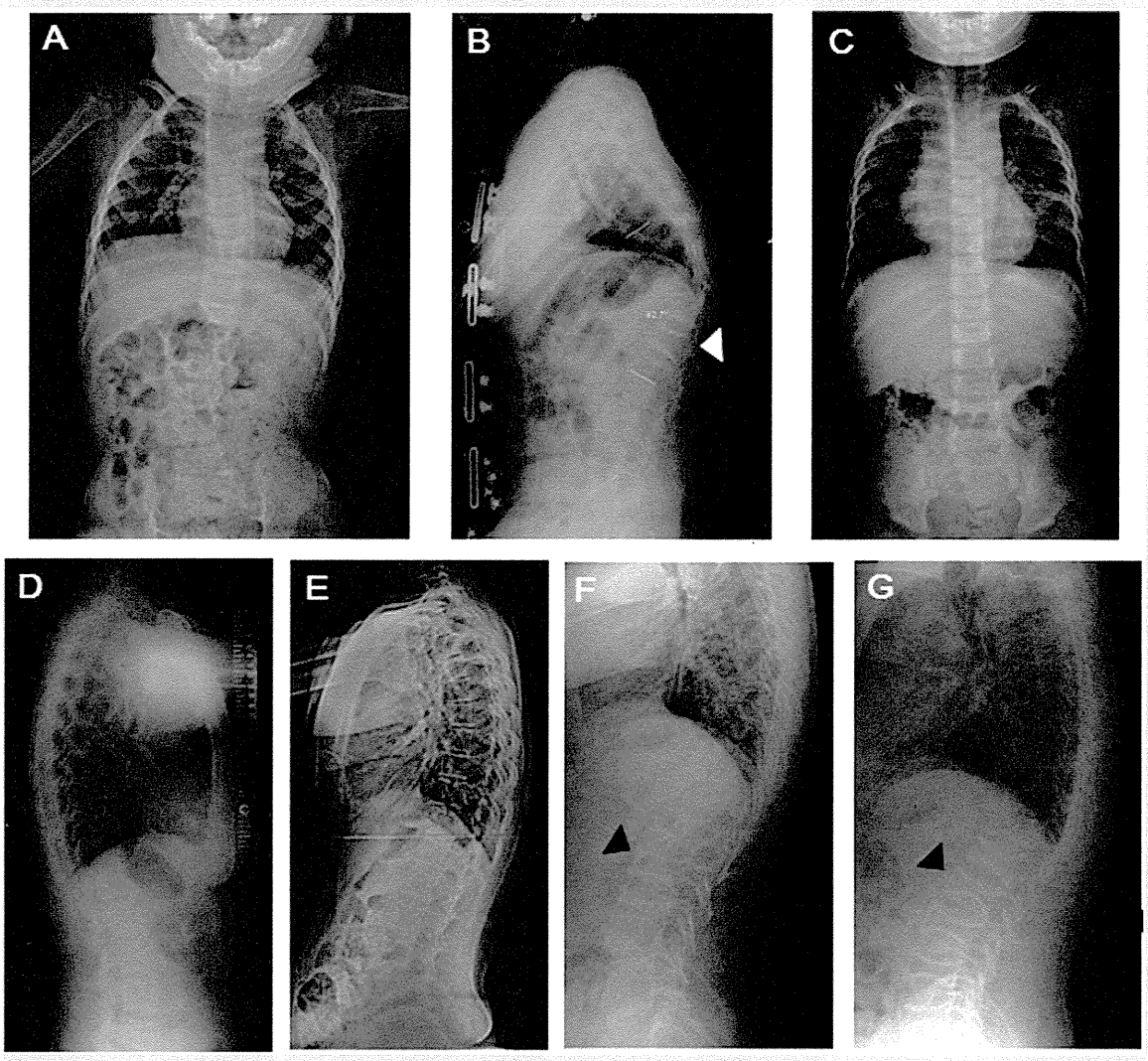

FIG. 3. Radiographs of the spine. A: Patient 1 at 2 years and 4 months of age. B: Patient 2 at 14 years of age. Osteoporosis with vertebral compression was indicated by white arrow heads. C: Patient 3 at 2 years of age. D: Patient 4 at 31 years of age. E: Patient 5 at 41 years of age. Patient 6 at 20 years of age (F) and his mother, Patient 7 at 46 years of age (G) showed biconcave shape of compression fractures [black arrow heads].

0.384 g/cm^2, corresponding to a T score of −6.1 and osteoporosis was evident.

Patient 7

Patient 7 is Korean woman, who is currently 46 years of age and is an affected mother of Patient 6. She was examined after her son was found to have an abnormality during mutation analysis. She shared similar facial features with her son. Her height was 150 cm (10th centile of Korean females). She experienced premature loss of the molar teeth and received implanted dentures at 40 years of age. She had longstanding back pain but received no further investigation. A skeletal survey detected Wormian bones in the lambdoidal suture, platybasia, marked compression fractures throughout the lumbar spine, and generalized osteoporosis (Fig. 3G). However, she did not present with acroosteolysis in her hands.

Mutation Analysis

After obtaining informed consent, genomic DNA was isolated from the peripheral leukocytes of the patients. Each exon and the flanking intronic sequences of *NOTCH2* were amplified using primers based on GenBank sequences (Supplementary eTable I—see Supporting Information online, GenBank accession number: NC_000001.10). The M13 reverse or forward sequence was added to the 5′ end of the polymerase chain reaction (PCR) primers and used as a sequencing primer. After purification, the PCR samples were directly sequenced using the ABI BigDye terminator Cycle Sequencing Kit (Applied Biosystems, Foster City, CA). Reactions were run

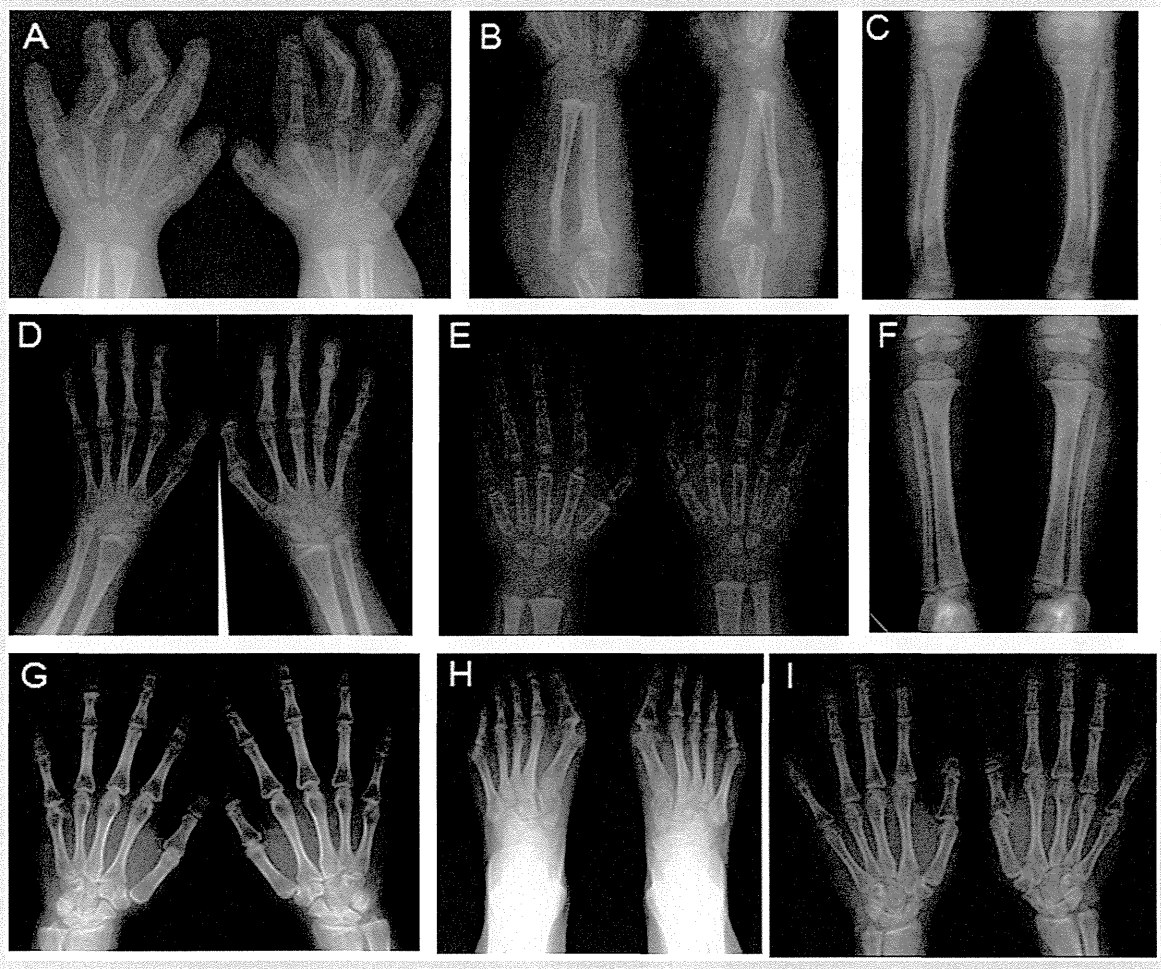

FIG. 4. Radiographs of the hands and feet. Patient 1 showed acroosteolysis of both the second and fifth fingers along with slender short tubular bones (A), twisted radii with proximal radioulnar dislocation (B), bowed tibiae and serpentine fibulae (C). Patient 2 at 14 years of age; acroosteolysis of the distal phalanges evident (D). Patient 3 at 2 years of age showing no acroosteolysis (E), and mild bowing tibiae (F). Bilaterally symmetrical acroosteolysis in distal phalanges was shown in Patient 4 (G/H) and Patient 6 (I).

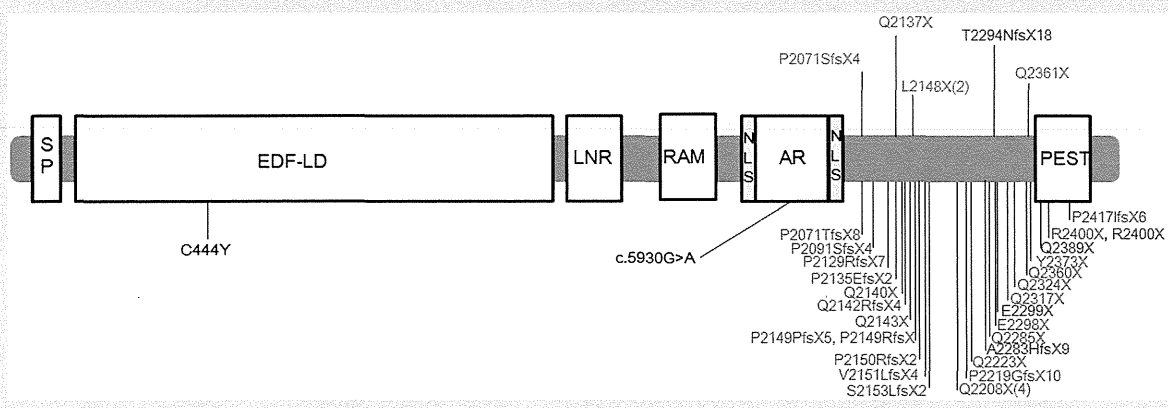

FIG. 5. Domain organization and identified *NOTCH2* mutations in HCS (red letter), SFPKS (blue letter), and Alagille syndrome (black letter). The mutations detected in this study are shown above the domain structure. The figures in parenthesis indicate the number of families. The functional domains are indicated as follows: SP, signal peptide; EDF-LD, EGF-like domain; LNR, Lin-Notch repeat; RAM, RAM 23 domain; NLS, nuclear localization signal; AR, Ankyrin repeats; PEST, proline-glutamic acid-serine-threonine-rich domain.

TABLE I. Characteristics of 34 Patients With NOTCH2 Mutations

	Patient 1	Patient 2	Patient 3	Patient 4	Patient 5	Patient 6	Patient 7	23 Patients with HCS and NOTCH2[a]	4 Patients with SFPKS and NOTCH2[b]	Total 34 patients with NOTCH2 (%)	Frequency in HCS[c] (%)
Gender	F	F	F	F	F	M	F				
Age	2	14	2	31	41	20	46				
Nucleotide	c.6883_6884ins A	c.7081C>T	c.6409G>T	c.6190_6212dup	c.6428T>C	c.6428T>C	c.6428T>C				
Protein	p.Thr2294AsnfsX18	p.Gln2361X	p.Glu2137X	p. Pro2071AsnfsX4	p.Leu2148X	p.Leu2148X	p.Leu2148X				
Inheritance	De novo	De novo	De novo	De novo	De novo	Familial	Familial				
Craniofacial Findings											
Synophrys	−	+	+	+	+	+	+	11/11	1/3	86 (18/21)	46
Midfacial flattening	+	+	+	+	+	+	+	1/3	0/3	62 (8/13)	32
Downslanted palpebral fissures	−	+	+	+	+	+	+	14/14	0/3	83 (20/24)	21
Hypertelorism	+	+	−	+	+	+	+	23/23	2/3	94 (31/33)	37
Wide nose	+	+	+	−	+	+	+	14/14	1/3	88 (21/24)	39
Long philtrum	+	+	+	−	+	+	+	23/23	3/4	94 (32/34)	40
Thin lips	+	+	+	+	+	+	+	2/2	2/3	92 (11/12)	n.d.
Low set ears	+	+	−	−	+	+	+	23/23	4/4	94 (32/34)	26
Retro/micrognathia	+	+	+	+	+	+	−	19/23	4/4	85 (29/34)	56
Coarse hair	+	+	−	+	+	+	+	1/1	n.d.	88 (7/8)	28
Coarse/dry skin	−	+	−	+	+	+	−	n.d.	1/1	75 (6/8)	7
Abnormal dentition	+	+	−	+	+	−	+	16/23	3/4	71 (24/34)	67
Hearing impairment	+	+	−	−	−	−	−	9/11	4/4	68 (15/22)	33
Congenital heart defect	+	+	+	−	+	−	−	3/23	4/4	32 (11/34)	12
Polycystic kidneys	+	−	−	−	−	−	−	4/22	3/4	24 (8/33)	14
Short stature	+	+	+	−	+	−	−	10/22	3/4	52 (17/33)	51
Developmental delay	+	+	−	−	−	−	−	0/12	1/4	13 (3/23)	18
Radiographic findings											
Acroosteolysis hands and feet	+	+	−	+	+	+	−	21/23	1/4	79 (27/34)	84
Womian bone	+	+	+	+	+	+	+	12/12	2/3	95 (21/22)	67
Platybasia/basilar impression	−	+	−	−	+	+	+	8/12	1/3	59 (13/22)	53
Osteoporosis	+	+	−	−	+	+	+	19/23	3/4	79 (27/34)	60
Fibular bowing	+	+	−	−	−	−	−	1/12	4/4	30 (7/23)	9
Spinal compression/ fracture	−	+	−	−	+	+	+	9/23	0/4	38 (13/34)	49
Fracture of long bones	+	+	−	−	−	−	−	0/3	1/4	21 (3/14)	28

[a]Marik et al. [2006], McKiernan [2007], Isidor et al. [2011a], Majewski et al. [2011].
[b]Majewski et al. [1993], Rosser et al. [1996], Albano et al. [2007], Gray et al. [2012], Isidor et al., [2011b].
[c]Brennan and Pauli [2001].

on an ABI 3100 semi-automated sequencing analyzer (Applied Biosystems). The DNA sequences were analyzed using FinchTV version 1.4.0 (Geospiza, Inc., Seattle, WA).

All patients had heterozygous, truncating mutations in exon 34 of *NOTCH2*. Patient 1 had c.6883_6884 ins A (p. Thr2294Asn fsX18), Patient 2 c.7081C>T (p.Gln2361X), Patient 3 c.6409 G>T (p. Glu2137X), and Patient 4 c.6190_6212dup (p.Pro2071AsnfsX4; Supplementary eFig. 1—see Supporting Information online). These mutations were previously unreported. Patients 5–7 had a recurrent mutation, c.6428T>C (p.Leu2148X).

DISCUSSION

In this study, we analyzed six HCS patients and one SFPKS patient with heterozygous mutations in *NOTCH2*. In previous reports on 48 patients from the 36 families, all patients had premature termination mutations in exon 34 (Fig. 5). All known HCS- or SFPKS-related *NOTCH2* mutations are dispersed throughout exon 34. Even the most common recurrent mutation (Gln2208X) was found only in four of the 36 families. In our series, we found Thr2294Asn fsX18 caused SFPKS, Gln2361X caused severe HCS with serpentine fibula, and Pro2071AsnfsX4 caused mild HCS. The patient with Glu2137X was too young to verify the final skeletal phenotype. It seems impossible to predict the clinical outcome from the mutation site.

Table I summarizes clinical and radiological manifestations in our series and all previously reported patients with *NOTCH2* mutations whose clinical manifestations are available (29 patients with HCS and five patients with SFPKS) [Majewski et al., 1993, 2011; Rosser et al., 1996; Marik et al., 2006; Albano et al., 2007; McKiernan, 2007; Isidor et al., 2011a,b; Gray et al., 2012]. We found 13 manifestations including synophrys, downslanted palpebral fissures, hypertelorism, wide nose, long philtrum, thin lips, low set ears, retro/micrognathia, coarse hair, coarse/dry skin, acroosteolysis, Wormian bones, and osteoporosis in >75% of *NOTCH2*-positive patients. Acroosteolysis is a characteristic clinical feature of HCS that usually develops during late childhood or adolescence [Brennan and Pauli, 2001]. Patient 7, 46 years of age, did not present acroosteolysis. However, acroosteolysis and osteoporosis with recurrent fractures were noted during infancy in Patient 1. In SFPKS patients, we observed the characteristic manifestations of HCS noted by Brennan et al. in their study including retro/micrognathia in five patients; abnormal dentition and short stature in four; Wormian bone in three; mid-facial flattening, coarse hair, and platybasia in one. In contrast, hearing impairment was observed in 10 HCS patients, polycystic kidneys in 4, and fibula bowing in 2. Serpentine fibula was observed in Patient 2, who developed unusually severe osteoporosis during adolescence. Thus, Patient 2 was considered to have an intermediate severity between HCS and SFPKS. These results suggest that truncating mutations in exon 34 of *NOTCH2* would cause a disorder, mainly characterized by abnormal bone turnover with various degrees of severity and occasionally accompanied by craniofacial features, cardiac, and renal defects.

In conclusion, clinical and molecular data in our series and previously reported patients suggest that HCS and SFPKS are a single disorder with variable degree of expression. This variability may be related to other modifier effects on possible truncating mutations in exon 34 of *NOTCH2*. Further analysis is needed to elucidate the pathogenesis of truncating mutation in exon 34 of *NOTCH2* on bone metabolism as well as various systems.

ACKNOWLEDGMENTS

The authors appreciate the patients and their families for their cooperation. We are also thankful to Tomomi Yamaguchi for her technical assistance.

REFERENCES

Albano LM, Bertola DR, Barba MF, Valente M, Robertson SP, Kim CA. 2007. Phenotypic overlap in Melnick-Needles, serpentine fibula-polycystic kidney and Hajdu-Cheney syndromes: A clinical and molecular study in three patients. Clin Dysmorphol 16:27–33.

Brennan AM, Pauli RM. 2001. Hajdu-Cheney syndrome: Evolution of phenotype and clinical problems. Am J Med Genet 100:292–310.

Currarino G. 2009. Hajdu-Cheney syndrome associated with serpentine fibulae and polycystic kidney disease. Pediatr Radiol 39:47–52.

Exner GU. 1988. Serpentine fibula-polycystic kidney syndrome. A variant of the Melnick-Needles syndrome or a distinct entity? Eur J Pediatr 147: 544–546.

Gray MJ, Kim CA, Bertola DR, Arantes PR, Stewart H, Simpson MA, Irving MD, Robertson SP. 2012. Serpentine fibula polycystic kidney syndrome is part of the phenotypic spectrum of Hajdu-Cheney syndrome. Eur J Hum Genet 20:122–124.

Han EJ, Mun JI, An SY, Jung YJ, Kim OH, Chung YS. 2010. A case report of Hajdu-Cheney syndrome. Endocrinol Metab 25:152–156[Korean].

Hwang S, Shin DY, Moon SH, Lee EJ, Lim SK, Kim OH, Rhee Y. 2011. Effect of zoledronic acid on acro-osteolysis and osteoporosis in a patient with Hajdu-Cheney syndrome. Yonsei Med J 52:543–546.

Isidor B, Lindenbaum P, Pichon O, Bézieau S, Dina C, Jacquemont S, Martin-Coignard D, Thauvin-Robinet C, Le Merrer M, Mandel JL, David A, Faivre L, Cormier-Daire V, Redon R, Le Caignec C. 2011. Truncating mutations in the last exon of *NOTCH2* cause a rare skeletal disorder with osteoporosis. Nat Genet 43:306–308.

Isidor B, Le Merrer M, Exner GU, Pichon O, Thierry G, Guiochon-Mantel A, David A, Cormier-Daire V, Le Caignec C. 2011. Serpentine fibula-polycystic kidney syndrome caused by truncating mutations in *NOTCH2*. Hum Mutat 32:1239–1242.

Kaplan P, Ramos FJ, Zackai EH, Bellah RD, Kaplan BS. 1995. Cystic kidney disease in Hajdu-Cheney syndrome. Am J Med Genet 56:25–30.

Majewski F, Enders H, Ranke MB, Voit T. 1993. Serpentine fibula-polycystic kidney syndrome and Melnick-Needles syndrome are different disorders. Eur J Pediatr 152:916–921.

Majewski J, Schwartzentruber JA, Caqueret A, Patry L, Marcadier J, Fryns JP, Boycott KM, Ste-Marie LG, McKiernan FE, Marik I, Van Esch H, FORGE Canada Consortium, Michaud JL, Samuels ME. 2011. Mutations in *NOTCH2* in families with Hajdu-Cheney syndrome. Hum Mutat 32:1114–1117.

Marik I, Kuklik M, Zemkowa D, Kozlowski K. 2006. Hajdu-Cheney syndrome: Report of a family and a short literature review. Sustralas Radiol 50:534–538.

McKiernan FE. 2007. Integrated anti-remodeling and anabolic therapy for the osteoporosis of Hjdu-Cheney syndrome. Osteoporos Int 18:245–249.

Ramos FJ, Kaplan BS, Bellah RD, Zackai EH, Kaplan P. 1998. Further evidence that the Hajdu-Cheney syndrome and the "serpentine

fibula-polycystic kidney syndrome" are a single entity. Am J Med Genet 78:474–481.

Rosser EM, Mann NP, Hall CM, Winter RM. 1996. Serpentine fibula syndrome: Expansion of the phenotype with three affected siblings. Clin Dysmorphol 5:207–212.

Simpson MA, Irving MD, Asilmaz E, Gray MJ, Dafou D, Elmslie FV, Mansour S, Holder SE, Brain CE, Burton BK, Kim KH, Pauli RM, Aftimos S, Stewart H, Kim CA, Holder-Espinasse M, Robertson SP, Drake WM, Trembath RC. 2011. Mutations in *NOTCH2* cause Hajdu-Cheney syndrome, a disorder of severe and progressive bone loss. Nat Genet 43:303–305.

Takatani R, Someya T, Kazukawa I, Nishimura G, Minagawa M, Kohno Y. 2009. Hajdu-Cheney syndrome: Infantile onset of hydrocephalus and serpentine fibulae. Pediatr Int 51:831–833.

Zanotti S, Canalis E. 2012. Notch regulation of bone development and remodeling and related skeletal disorders. Calcif Tissue Int 90:69–75.

Anal Bioanal Chem (2013) 405:1345–1351
DOI 10.1007/s00216-012-6532-3

ORIGINAL PAPER

Intracellular in vitro probe acylcarnitine assay for identifying deficiencies of carnitine transporter and carnitine palmitoyltransferase-1

Jamiyan Purevsuren · Hironori Kobayashi · Yuki Hasegawa · Kenji Yamada · Tomoo Takahashi · Masaki Takayanagi · Toshiyuki Fukao · Seiji Fukuda · Seiji Yamaguchi

Received: 24 July 2012 / Revised: 10 October 2012 / Accepted: 30 October 2012 / Published online: 10 November 2012

Abstract Mitochondrial fatty acid oxidation (FAO) disorders are caused by defects in one of the FAO enzymes that regulates cellular uptake of fatty acids and free carnitine. An in vitro probe acylcarnitine (IVP) assay using cultured cells and tandem mass spectrometry is a tool to diagnose enzyme defects linked to most FAO disorders. Extracellular acylcarnitine (AC) profiling detects carnitine palmitoyltransferase-2, carnitine acylcarnitine translocase, and other FAO deficiencies. However, the diagnosis of primary carnitine deficiency (PCD) or carnitine palmitoyltransferase-1 (CPT1) deficiency using the conventional IVP assay has been hampered by the presence of a large amount of free carnitine (C0), a key molecule deregulated by these deficiencies. In the present study, we developed a novel IVP assay for the diagnosis of PCD and CPT1 deficiency by analyzing intracellular ACs. When exogenous C0 was reduced, intracellular C0 and total AC in these deficiencies showed specific profiles clearly distinguishable from other FAO disorders and control cells. Also, the ratio of intracellular to extracellular C0 levels showed a significant difference in cells with these deficiencies compared with control. Hence, intracellular AC profiling using the IVP assay under reduced C0 conditions is a useful method for diagnosing PCD or CPT1 deficiency.

Keywords Fatty acid oxidation · Carnitine cycle disorder · Acylcarnitine profile · ESI-MS/MS

J. Purevsuren · H. Kobayashi · Y. Hasegawa · K. Yamada · T. Takahashi · S. Fukuda · S. Yamaguchi (✉)
Department of Pediatrics, Shimane University School of Medicine, 89-1 Enya,
Izumo, Shimane 693-8501, Japan
e-mail: seijiyam@med.shimane-u.ac.jp

M. Takayanagi
Division of Metabolism, Chiba Children's Hospital,
Chiba 266-0007, Japan

T. Fukao
Department of Pediatrics, Graduate School of Medicine,
Gifu University,
Gifu, Gifu 501-1194, Japan

T. Fukao
Medical Information Sciences Division, United Graduate School of Drug Discovery and Medical Information Sciences,
Gifu University,
Gifu, Gifu 501-1194, Japan

J. Purevsuren
Medical Genetics Laboratory,
National Center for Maternal and Child Health,
Khuvisgalchdyn street, Bayangol district,
Ulaanbaatar 210624, Mongolia

Introduction

L-Carnitine plays an essential role in the transfer and activation of long-chain fatty acids across the outer and inner mitochondrial membranes during which it is acted upon by enzymes including carnitine transporter (OCTN2), carnitine palmitoyltransferase-1 (CPT1), carnitine palmitoyltransferase-2 (CPT2), and carnitine acylcarnitine translocase (CACT) (Fig. 1) [1, 2]. Carnitine penetrates into cells across the plasma membrane against a high concentration gradient of free carnitine with the aid of the plasma membrane OCTN2 protein encoded by the SLC22A5 gene [3]. Deficiency of OCTN2 causes primary carnitine deficiency (PCD, OMIM 212140), which is characterized by systemic carnitine deficiency in tissues and blood but in concord with increased excretion of free L-carnitine in the urine [4–6]. Clinical symptoms in patients with PCD such as cardiomyopathy,